Lognormal approximations to LIBOR market models

O. Kurbanmuradov * K. Sabelfeld † J. Schoenmakers ‡

July, 11, 2000

Mathematics Subject Classification: 60H10,65C05,90A09
Keywords: LIBOR interest rate models, random field simulation, Monte Carlo simulation of stochastic differential equations.

The authors would like to thank Hermann Haaf (Dresdner Kleinwort Benson) for helpful comments.

*Sci.Tech. Center *Climate* Turkmenian Hydrometeorology Comm., Azadi 81, 744000, Ashgabad, Turkmenistan, E-mail: seid@climat.ashgabad.su

†Institute of Computational Mathematics and Mathematical Geophysics, Russian Acad. Sciences, Akad. Lavrentieva, 6, 630090, Novosibirsk, Russia, E-mail: karl@osmf.sscc.ru and Weierstraß-Institut für Angewandte Analysis und Stochastik, Mohrenstraße 39, 10117, Berlin, E-mail: sabelfel@wias-berlin.de

‡Weierstrass Institute, Mohrenstrasse 39, D-10117 Berlin, E-mail: schoenma@wias-berlin.de

Abstract

We study several lognormal approximations for LIBOR market models, where special attention is paid to their simulation by direct methods and lognormal random fields. In contrast to conventional numerical solution of SDE's this approach simulates the solution directly at a desired point in time and therefore may be more efficient. As such the proposed approximations provide valuable alternatives to the Euler method, in particular for long dated instruments. We carry out a path-wise comparison of the different lognormal approximations with the 'exact' SDE solution obtained by the Euler scheme using sufficiently small time steps. Also we test approximations obtained via numerical solution of the SDE by the Euler method, using larger time steps. It turns out that for typical volatilities observed in practice, improved versions of the lognormal approximation proposed by Brace, Gatarek and Musiela, [2], appear to have excellent path-wise accuracy. We found out that this accuracy can also be achieved by Euler stepping the SDE using larger time steps, however, from a comparative cost analysis it follows that, particularly for long maturity options, the latter method is more time consuming than the lognormal approximation. We conclude with applications to some example LIBOR derivatives.

1 Introduction

By far the most important class of traded interest rate derivatives is constituted by derivatives which are specified in terms of *forward LIBOR rates*. The forward LIBOR[1] rate L is defined as the annualized effective interest rate over a forward period $[T_1, T_2]$ and can be expressed in terms of two zero-coupon bonds B_1 and B_2 with face value \$1, maturing at T_1 and T_2, respectively,

$$L(t; T_1, T_2) := \frac{\frac{B_1(t)}{B_2(t)} - 1}{T_2 - T_1}, \tag{1}$$

where as usual T_2 is the settlement date for the accrual LIBOR period. In several papers such as Brace, Gatarek and Musiela [2], Jamshidian [4], Musiela and Rutkowski, [7] arbitrage free models for the LIBOR rate process are constructed in order to price LIBOR derivatives such as caps, swaptions and more complicated types, so called exotics, in a direct way. For instance, in [2] the dynamics of the continuous family of processes $\{L(t, T, T+\delta) \mid T \geq 0,\ 0 \leq t \leq T\}$ is studied for a fixed $\delta > 0$, whereas Jamshidian [4] considered the processes $\{L_i(t) := L(t, T_i, T_{i+1}) \mid t \leq T_i,\ i = 1, \ldots, n-1\}$ for a discrete set of tenors $\{T_1, \ldots, T_n\}$. In both approaches special attention is paid to so called *LIBOR market models* which are models where for every settlement date the LIBOR process has deterministic volatility. Also in Schoenmakers and Coffey, [10], Sidenius, [12], applications of LIBOR market models are studied extensively. In a market model, each LIBOR is a *log-normal* martingale under the numeraire measure given by the bond which terminates at the LIBOR's settlement date.

In this paper we concentrate on a LIBOR market model for a discrete set of tenors given by a stochastic differential equation (SDE) in the terminal bond measure as developed in Jamshidian [4], equipped with a special correlation structure (2) presented below. For this model we have constructed lognormal approximations, efficient simulation methods for these approximations and outlined the application of the different simulation methods in various valuation problems in practice. The lognormal approximations, derived in section (2), are subjected in section (2.2) to mutual path-wise comparison and path-wise comparison with approximations obtained by Euler stepping the SDE. A ranking between the different approximations is thus obtained.

[1] LIBOR stands for London Inter Bank Offer Rate.

The main advantage of log-normal approximations is that their distributions can be simulated very fast, and, since the valuation of a LIBOR derivative generally comes down to the computation of the expected value of a function of LIBORs, an important family of LIBOR instruments, consisting of long dated products and in particular European style exotics, can be valuated faster by using lognormal approximations. As an example, the lognormal approximation of Brace, Gatarek and Musiela, [2], can be simulated effectively by a Gaussian random field of log-LIBORs. The efficiency of the proposed lognormal approximations with respect to Euler stepping SDE is analysed in section (4) and the results have led to an "optimal" simulation program presented in section (4.1). In section (5) we consider the valuation of swaptions and trigger swaps and compare the results for different approximations. Also we discuss briefly the callable reverse floater, an exotic instrument for which the proposed simulation method is extremely efficient.

For the simulation analysis in section (2) and the valuation examples in (5) we used a LIBOR market model with a full rank instantaneous correlation structure of the form

$$\rho_{ij} = \frac{\min(b_i, b_j)}{\max(b_i, b_j)}. \tag{2}$$

In (2) the sequence (b_i) is required to be positive, strictly increasing, and such that the sequence (b_i/b_{i+1}) is strictly increasing also. Further, it is clear that we may take $b_1 = 1$ without restriction. As such, the correlation structure (2) constitutes a full rank positive definite matrix, see Curnow, Dunnett, [3] and is proposed for the LIBOR model earlier by Schoenmakers and Coffey [10, 11]. The advantage of the structure (2) is, on one hand, that the number of parameters to be determined in the market model is, in a sense, the same as in the case of a two factor model and, on the other hand, as turned out in practice, that calibration of a market model based on (2) to the cap/swaption market is very stable and implies a system of LIBOR correlations which is well in accordance with the behaviour of statistically estimated correlations from historical data. In particular, the increasingness of b_i/b_{i+1} implies that instantaneous correlations $\rho(dL_i, dL_{i+p})$ are increasing in i for fixed p, which is very natural indeed. See, e.g. the historical correlation table 0 in [2] and Schoenmakers and Coffey [10, 11], for further discussion of this issue. Moreover, it appeared in many cases that, for a sequence (b_i) calibrated to the cap/swap market, by linear regression on the pairs $(\ln\ln b_i, \ln(i-1))$; $i > 1$, the structure (2) is very well fitted by a simple two parametric function, for instance

$$b_i = \exp[\beta(i-1)^\alpha]; \quad \beta > 0,\ 0 < \alpha < 1. \tag{3}$$

In fact, there are many more suitable parsimonious parametrizations possible for a correlation structure of the form (2) and in [11] such parametrizations are derived in a systematic way. Another appealing feature of a simple multi-factor correlation structure such as (2) combined with (3) is that, once (2) is calibrated, one can choose a specific low number of factors, e.g. two, three or four and then consider only the first two, three or four principal components of (2), respectively. One thus yields a low factor model that is calibrated in a stable way. If necessary, one can fine tune this low factor model again by, for instance, re-calibration via a deterministic volatility norm function which is specified by a properly chosen functional specification. See [11] and the references therein for more details. In this paper we implemented (3) as example correlation structure.

2 Different log-normal approximations

For a given tenor structure $0 < T_1 < T_2 < \ldots < T_n$ we consider a Jamshidian LIBOR market model [4] for the forward LIBOR processes L_i in the terminal bond numeraire $\mathbb{P}_n$,

$$dL_i = -\sum_{j=i+1}^{n-1} \frac{\delta_j L_i L_j \, \gamma_i \cdot \gamma_j}{1+\delta_j L_j}\, dt + L_i \, \gamma_i \cdot dW^{(n)}, \tag{4}$$

where, for $i = 1, \ldots, n-1$, the L_i are defined in the intervals $[t_0, T_i]$, $\delta_i = T_{i+1} - T_i$ and $\gamma_i = (\gamma_{i,1}, \ldots, \gamma_{i,d})$ are given deterministic functions, called factor loadings, defined in $[t_0, T_i]$, respectively. In (4), $(W^{(n)}(t) \mid t_0 \le t \le T_{n-1})$ is a standard d-dimensional Wiener process under $\mathbb{P}_n$, where $d \le n-1$. In case of a full rank correlation structure such as (2), however, we need $d = n-1$ Wiener processes. It is convenient to deal with the following integral form of (4):

$$\ln \frac{L_i(t)}{L_i(t_0)} = -\int_{t_0}^{t} \sum_{j=i+1}^{n-1} \frac{\delta_j L_j |\gamma_i||\gamma_j| \rho_{ij}}{1+\delta_j L_j}\, ds - \frac{1}{2}\int_{t_0}^{t} |\gamma_i|^2 ds + \int_{t_0}^{t} \gamma_i \cdot dW^{(n)}, \tag{5}$$

where $\rho_{ij} = \gamma_i \cdot \gamma_j \, / |\gamma_i||\gamma_j|$. In practice, we may define the vectors $\gamma_i/|\gamma_i|$ through the matrix (ρ_{ij}) by applying a Cholesky decomposition.

Note that only the first term in the right hand side of (5) is generally non-Gaussian. Let us consider the contribution of the non-Gaussian term where we assume for simplicity that the functions γ_i are constants. We introduce the notations: $\rho_i = \sum_{j=i+1}^{n-1} |\rho_{ij}|$, $\rho = \max_i \rho_i$, $\delta = \max_i \delta_i$, and $\gamma = \max_i |\gamma_i|$. Let us denote by $\tilde{L}$ the maximum value of the L_i, i.e., $\tilde{L} = \max_i \sup_{t_0 \le t \le T_i} L_i(t)$. Then, we may write (5) as

$$\ln \frac{L_i(t)}{L_i(t_0)} = \varepsilon_i - \frac{1}{2}|\gamma_i|^2 (t - t_0) + |\gamma_i| \sqrt{t - t_0}\, Z_i(t),$$

where $Z_i(t)$ is a standard normally distributed random variable and ε_i can be estimated by $|\varepsilon_i| \le (t - t_0)\delta \tilde{L} \gamma^2 \rho_i$. So, by neglecting ε_i we cause in L_i only a small *relative* error of order of ε_i when

$$|\varepsilon_i| \le (t - t_0)\delta \tilde{L} \gamma^2 \rho_i \le (t - t_0)\delta \tilde{L} \gamma^2 \rho << 1. \tag{6}$$

Note that for typical values, e.g., $\delta = 0.25$, $\gamma = 0.15$, $\tilde{L} = 0.07$, $t - t_0 = 10$, this relative error is about $0.4\rho\,\%$. However, dependent on ρ and the length of the tenor structure this error can become rather large in practice.

The approximation by neglecting the non-Gaussian terms ε_i in (5) will be called (0)−approximation to (4). With this approximation, forward LIBOR rates satisfy

$$dL_i^{(0)} = L_i^{(0)} \, \gamma_i \cdot dW^{(n)} \ , \tag{7}$$

and are given by the explicit solution

$$L_i^{(0)}(t) = L_i(t_0) \exp\left\{ -\frac{1}{2}\int_{t_0}^{t} \gamma_i^2(s) ds + \int_{t_0}^{t} \gamma_i(s) \cdot dW^{(n)}(s) \right\}. \tag{8}$$

Below we show for illustration (see Figs. 1,2) some typical samples of $L_i(t)$ and $L_i^{(0)}(t)$, where we chose $n = 31$ and relatively high volatility norms, $|\gamma_1| = \ldots = |\gamma_{n-1}| = 0.4$, in order to amplify effects. Further we take a correlation matrix ρ_{ij} given by (2), where

$$b_i = \exp[\beta(i-1)^\alpha]. \tag{9}$$

So the correlations are defined via two parameters, β and α, see also [10] and for our simulations, presented in the figures below, we took $\alpha = 0.8$, $\beta = 0.1$ and $\alpha = 0.8$, $\beta = 0.3$, respectively. Further we chose $t_0 = 0$ and a uniform tenor structure $T_i = i\delta$ with $\delta = 0.25$, $i = 1, \ldots, 31$. The initial L values were taken to be $L_i(0) = 0.061$. The 'true' process $L_i(t)$ is simulated by an Euler scheme with time discretization step $\delta/10$.

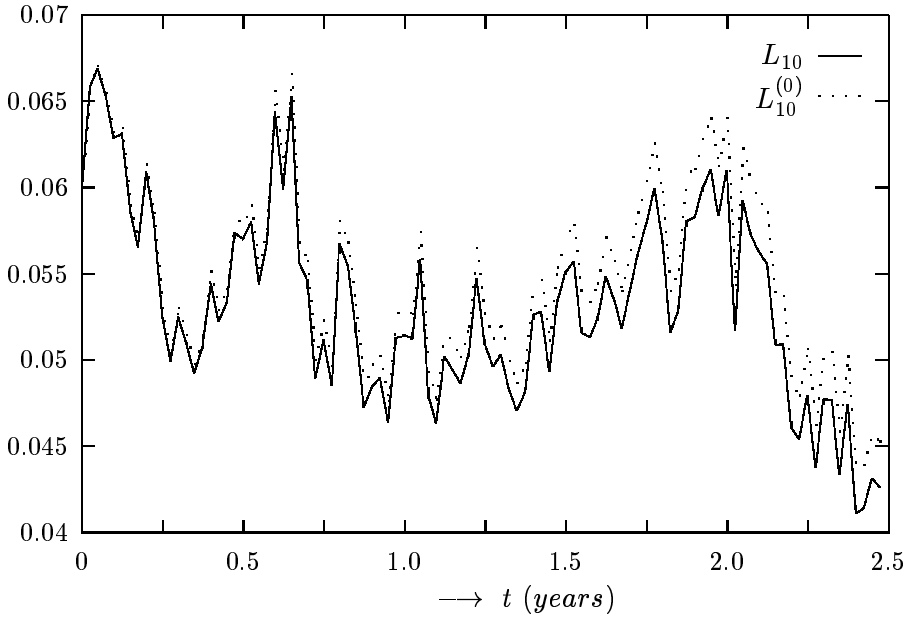

Fig.1 *A sample of* $L_{10}(t)$ *and* $L_{10}^{(0)}(t)$*, for* $\alpha = 0.8$ *and* $\beta = 0.1$.

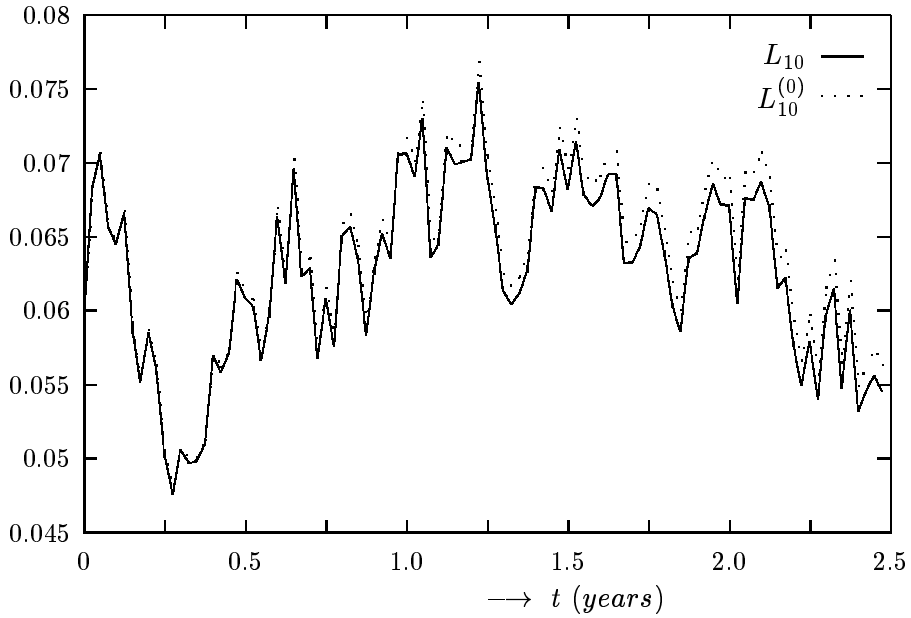

Fig.2 *A sample of* $L_{10}(t)$ *and* $L_{10}^{(0)}(t)$*, for* $\alpha = 0.8$ *and* $\beta = 0.3$.

From the trajectories presented in Figs.1-2 it is seen that on the initial time interval, the function $L_{10}^{(0)}$ approximates the function L_{10} very well. For increasing time, however, the discrepancy increases. Also for increasing ρ in (6), respectively decreasing β in (9), it is clear from (6) that the discrepancy increases. Both effects are illustrated by Figs.1-2 and their comparison.

So, from the pictures in Figs.1-2 we see that the (0)−approximation performs well for small times, whereas from (6) we see that for large i the (0)-approximation produces good results

also because ρ_i decreases with i (e.g., ρ_{n-1} vanishes). More details about the (0) and other approximations are presented in Tables 1-5.

In Fig.3 we show a sample for the bond price $B_{31}(T_i)$ and its (0)-approximation $B_{31}^{(0)}(T_i)$, $i = 0, \ldots, 31$ for the same model parameters as used for Fig.1. The bond prices are computed from the LIBOR process, via the relationship

$$B_{31}(T_i) = \prod_{j=i}^{30} (1 + \delta L_j(T_i))^{-1} \tag{10}$$

and a similar one for the (0)−approximations, where for the 'true' bond prices we have used 'true' LIBORs, simulated by an Euler scheme with time discretization step $\delta/10$.

In contrast to the results presented in Figs.1-2, the maximum discrepancy happens around the middle of the time interval $(0, T_{31})$. The reason is clear from (10). Indeed, either when i is close to zero or when i is close to 30 where the drift terms become small, the approximations $L_j^{(0)}(T_i)$, $j = i, \ldots, 30$ are close to $L_j(T_i)$ and so $B_{31}^{(0)}(T_i)$ is close to $B_{31}(T_i)$. Note that, exactly, $B_{31}^{(0)}(30 \times 0.25) = B_{31}(30 \times 0.25)$ because L_{30} and $L_{30}^{(0)}$ coincide in the terminal measure given by $n = 31$.

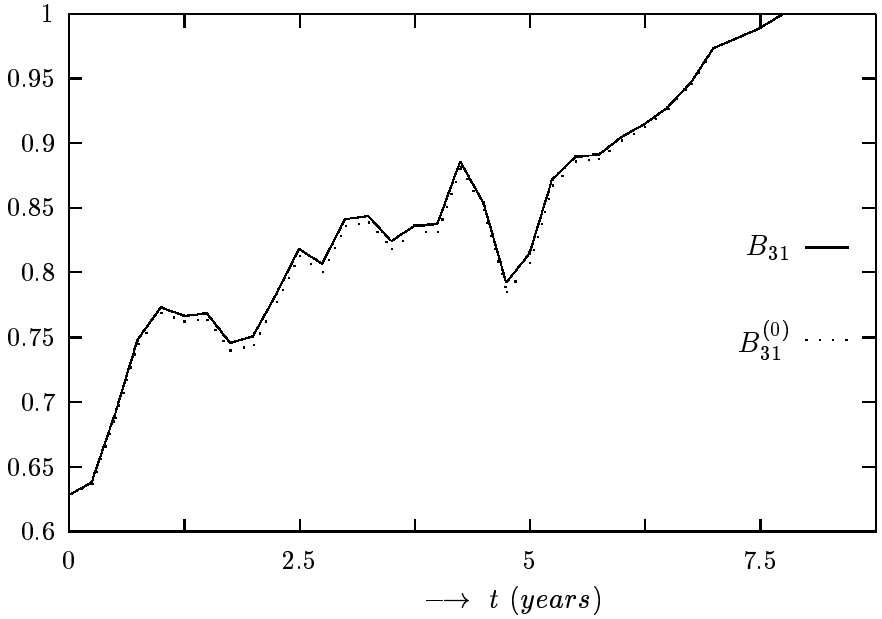

Fig.3 *A sample of Bond prices* $B_{31}(t)$ *and its* (0)*-approximation, for* $\alpha = 0.8$, $\beta = 0.1$, $n = 31$.

2.1 More lognormal approximations

It is of interest to consider more refined approximations to L and in particular to look for lognormal approximations improving $L^{(0)}$. So, in fact, we need to find a deterministic or normal approximation to the sum term in the integral representation (5). Therefore, for each j we approximate the process

$$Z_j(t) := \frac{\delta_j L_j}{1 + \delta_j L_j} \tag{11}$$

in the following way. Let the function f be defined as $f(x) := x/(1+x)$ and $Z_j = f(\delta_j L_j)$. Hence the process $Z := [Z_1, \ldots, Z_{n-1}]$ satisfies the SDE system

$$\begin{aligned} dZ_j &= f'(\delta_j L_j)\delta_j L_j \gamma_j \cdot dW^{(n)} + \frac{1}{2} f''(\delta_j L_j)[\delta_j L_j |\gamma_j|]^2 dt \\ &\quad - \sum_{k=j+1}^{n-1} \frac{\delta_j \delta_k L_j L_k \, \gamma_j \cdot \gamma_k}{1+\delta_k L_k} f'(\delta_j L_j) dt \qquad (12) \\ &= : a_j(Z,t)dt + b_j(Z,t) \cdot dW^{(n)}, \end{aligned}$$

with initial conditions $Z_j(t_0) = f(\delta_j L_j(t_0))$. Note that by solving (11) for the $L_j' s$ and substituting the result in (12) it is immediately clear how the coefficients a_j and b_j should be defined explicitly.

The Picard-Lindelof-0 and Picard-Lindelof-1 iteration for the solution of this SDE are

$$\begin{aligned} Z_j^{(0)}(t) &:\equiv Z_j(t_0) = \frac{\delta_j L_j(t_0)}{1+\delta_j L_j(t_0)} \qquad \text{and} \\ Z_j^{(1)}(t) &:= Z_j(t_0) + \int_{t_0}^t [a_j(Z^{(0)}(t_0), s)ds + b_j(Z^{(0)}(t_0), s) \cdot dW^{(n)}(s)] \\ &= f(\delta_j L_j(t_0)) + \frac{1}{2} f''(\delta_j L_j(t_0)) \delta_j^2 L_j^2(t_0) \int_{t_0}^t |\gamma_j|^2 ds \\ &\quad - \sum_{k=j+1}^{n-1} \frac{\delta_j \delta_k L_j(t_0) L_k(t_0)}{1+\delta_k L_k(t_0)} f'(\delta_j L_j(t_0)) \int_{t_0}^t \gamma_j \cdot \gamma_k ds \\ &\quad + f'(\delta_j L_j(t_0)) \delta_j L_j(t_0) \int_{t_0}^t \gamma_j \cdot dW^{(n)}(s), \qquad (13) \end{aligned}$$

so deterministic and Gaussian, respectively. The next Picard-Lindelof iteration, however, will be non-Gaussian in general.

By using the approximations $Z_j^{(0)}$ for the expression (11) in (5), we find a lognormal approximation which we call the $(g)-$ approximation,

$$\ln \frac{L_i^{(g)}(t)}{L_i(t_0)} = -\int_{t_0}^t \frac{|\gamma_i(s)|^2}{2} ds + \int_{t_0}^t \gamma_i(s) \cdot dW^n(s) - \sum_{j=i+1}^{n-1} \int_{t_0}^t \frac{\delta_j L_j(t_0) \gamma_i \cdot \gamma_j \ (s)}{1+\delta_j L_j(t_0)} ds \qquad (14)$$

which turns out to be a considerable path-wise improvement of the $(0)-$approximation and is suggested in [2]. See, e.g., also [10] for several applications. By expanding f, f' and f'' as $f(x) = x + \mathcal{O}(x^2)$, $f'(x) = 1 + \mathcal{O}(x)$ and $f''(x) = -2 + \mathcal{O}(x)$, respectively and denoting identity modulo terms of order $\mathcal{O}(\delta_j^2 L_j^2(t_0))$ by $\cong$, we have

$$\begin{aligned} Z_j^{(1)}(t) &\cong \delta_j L_j(t_0)(1 + \int_{t_0}^t \gamma_j \cdot dW^{(n)}(s)) - \sum_{k=j+1}^{n-1} \frac{\delta_j \delta_k L_k(t_0) L_j(t_0)}{1+\delta_k L_k(t_0)} \int_{t_0}^t \gamma_j \cdot \gamma_k(s) ds \qquad (15) \\ &=: \tilde{Z}_j(t). \end{aligned}$$

We note that, while in (15) the terms in the sum are of order $\mathcal{O}(\delta_j^2 L_j^2(t_0))$, their sum is possibly of order $\mathcal{O}(\delta_j L_j(t_0))$ and therefore not neglected. Now, by substituting $\tilde{Z}$ for (11) in (5) we get another lognormal approximation, the $(g1)-$approximation,

$$\ln \frac{L_i^{(g1)}(t)}{L_i(t_0)} = -\sum_{j=i+1}^{n-1} \int_{t_0}^t \tilde{Z}_j(s) \gamma_i \cdot \gamma_j \ (s) ds - \frac{1}{2} \int_{t_0}^t |\gamma_i(s)|^2 ds + \int_{t_0}^t \gamma_i(s) \cdot dW^{(n)}(s),$$

The $(g1)-$approximation in its turn improves the $(g)-$approximation significantly as will appear from a comparative analysis in (2.2). We will also test a simplification of the $(g1)-$approximation: the $(g1')-$approximation, which is obtained by neglecting the sum-term in (15).

Finally, by substituting $Z^{(1)}$ for (11) in (5), so without linearization of the function f and its first and second derivative, we get a next refinement, the $(g2)-$approximation, given by

$$\ln \frac{L_i^{(g2)}(t)}{L_i(t_0)} = -\sum_{j=i+1}^{n-1} \int_{t_0}^{t} Z_j^{(1)}(s)\gamma_i \cdot \gamma_j\ (s)ds - \frac{1}{2}\int_{t_0}^{t} \gamma_i^2(s)ds + \int_{t_0}^{t} \gamma_i(s) \cdot dW^{(n)}(s),$$

where $Z^{(1)}$ is given by (13).

2.2 Numerical simulation analysis

It is now interesting to carry out a comparative numerical analysis of the different lognormal approximations: For typical market volatilities we will compare the lognormal approximations path-wise with the 'true' solution, obtained by solving the stochastic differential equation (4) by the Euler method using small time steps. Besides, we will carry out a comparison of (non-lognormal) approximations obtained by the Euler scheme using larger time steps. For a uniform tenor structure we will experiment with Euler steps equal δ, 2δ or 3δ, etc.

For a correct path-wise comparison, we construct all the lognormal approximations in one common probability space by solving their accompanying stochastic differential equations by the Euler scheme with small time steps, namely, the time steps used for the 'true' solution. In the numerical schemes, this is easily achieved by using one and the same Wiener increments for all approximations. In fact, we will solve the SDE's for the $\log-$LIBORs and their approximations rather than the LIBORs as we attain in this way a path-wise accuracy of order *one* with the Euler scheme, due to the deterministic diffusion coefficients in the several $\log-$LIBOR SDE's. The different SDE's for the $\log-$LIBORs are straightforwardly obtained by taking the differential form of (14), (16) and (17), respectively.

In our next experiments we take $n = 61$ and $\delta_i = 0.25$, i.e. a rather large tenor structure of fifteen years, further the same initial conditions as used for the generation of Figs 1,2: $L_i(0) = 0.061$. We take for European markets relatively high but still realistic volatility norms, $|\gamma_i| = 0.15$ and for the correlation structure (3) we take $\alpha = 0.9$ and $\beta = 0.04$, yielding a more or less realistic correlation table 0. For comparison see, e.g., table 4.2. in [2]. Note that the off-diagonals in table 0 are slightly increasing. The "true" solution is simulated by the Euler method using $\Delta t = \delta/5$.[2] In tables 1,2,3,4 it is shown how often the relative error (in percents) of the corresponding approximation to L_{12}, L_{24}, L_{36} and L_{48} lies in the relevant percentage intervals (of course there is no table for L_{60} because L_{60} is exactly lognormal in the terminal measure). The relative error between $\hat{L}_i$, the numerical solution to the original equation (4) and, for instance $\hat{L}_i^{(g)}$, the numerical solution to the SDE belonging to $(g)-$approximation is defined as

$$\epsilon_i^{(g)} = \max_{1\le j\le i} \frac{|\hat{L}_i(T_j) - \hat{L}_i^{(g)}(T_j)|}{\hat{L}_i(T_j)}. \tag{18}$$

The relative errors to other approximations are defined analogously.

The numbers in the columns 2 - 8 of table 1 show the number of samples out of 100 for which the event shown in the first column happens. Firstly, we conclude that the path-wise errors produced by the $(0)-$approximation are generally not tolerable, as almost every path

[2]For this choice of Δt it appeared by comparison with much smaller Δt that the discretization bias of the "true" solution is negligible w.r.t. the bias of the different approximations.

has an error in the sense of (18) of at least 2-3%. The $(g)-$approximation proposed by Brace et al. in [2] and used for their swaption approximation formula there, gives a considerable improvement but is clearly outperformed by the lognormal approximations $(g1')$ $(g1)$ and $(g2)$. For smaller to moderate $\epsilon's$, $(g2)$ appears to perform slightly better than $(g1)$ and in its turn $(g1)$ somewhat better than $(g1')$ as expected, however, for high ϵ (close to 100%) the reverse conclusion can be made which indicates that $(g2)$ produces higher outliers than $(g1)$ and so on. Obviously, the (non-lognormal) $\delta-$stepping Euler approximation appears to be the most accurate one, but, as we will see in section (3), is in many applications more expensive than the proposed lognormal approximations since the distributions of the latter may be simulated directly at the desired points in time by methods described in section (3). In addition, for the typical model parameters chosen in these experiments, we may conclude that the refined lognormal approximations are roughly comparable with $2\delta-$ or $3\delta-$stepping Euler while the implementation of the latter is in many situations less efficient, see for details section (3).

Remark 2.2.1 As the bias of different LIBOR approximations with respect to the terminal measure is caused by the approximation of the sum term in (5) we may expect that the larger this term is, the larger the bias will be. Particularly, this sum term tends to zero when $t \downarrow t_0$ and when $i \uparrow n-1$. For instance, in order to estimate roughly which $L_i(T_i)$ has the largest bias in a specific lognormal approximation, we may approximate the sum term in (5) by replacing the L_j by their initial values (like in the $(g)-$ approximation) and then obtain for the experiments in (2.2),

$$\ln \frac{L_i(T_i)}{L_i(0)} = \ln \frac{L_i(i\delta)}{L_i(0)} = \Sigma^{(i)} - \frac{1}{2}|\gamma|^2 i\delta + \int_0^{i\delta} \gamma_i \cdot dW^{(n)}, \quad \text{where}$$

$$\Sigma^{(i)} \approx -|\gamma|^2 \frac{\delta^2 L(0)}{1+\delta L(0)} \sum_{j=i+1}^{n-1} i \frac{e^{\beta(i-1)^\alpha}}{e^{\beta(j-1)^\alpha}} \tag{19}$$

and in the experiments, $L(0) = 0.061$, $\alpha = 0.9$ $\beta = 0.04$, $|\gamma| = 0.15$, $\delta = 0.25$, $n = 61$. Since in practice α is very close to 1, we now take $\alpha = 1$ in (19) for analytical tractability and then get

$$|\Sigma^{(i)}| \approx |\gamma|^2 \frac{\delta^2 L(0)}{1+\delta L(0)} \frac{1}{e^\beta - 1} i(1 - e^{-(n-1-i)\beta}).$$

Hence, for $\beta = 0$ (so, in fact, for a one-factor model), we have $|\Sigma^{(i_0^*)}| \approx |\gamma|^2 \frac{\delta^2 L(0)}{1+\delta L(0)} i(n-i-1)$, which has a maximum $|\Sigma^{(i_0^*)}| \approx |\gamma|^2 \frac{\delta^2 L(0)}{1+\delta L(0)} \frac{(n-1)^2}{4}$ for $i = i_0^* \approx \frac{n-1}{2}$, whereas for $\beta \uparrow \infty$ (full decorrelation) it follows by elementary analysis that the $|\Sigma|-$ maximum, say $|\Sigma^{(i_\beta^*)}|$, goes to zero while $i_\beta^* \to n-2$, non-decreasingly. In a particular situation, however, we can search numerically for i_β^* and for the experiments in (2.2) we thus find $i_{0.04}^* \approx 37$, which is more or less consistent with the results listed in tables 1-4.

i,j	4	8	12	16	20	24	28	32	36	40	44	48	52	56	60
4	1	0.88	0.79	0.7	0.63	0.57	0.51	0.46	0.42	0.38	0.34	0.31	0.28	0.26	0.23
8	0.88	1	0.89	0.8	0.71	0.64	0.58	0.52	0.47	0.43	0.39	0.35	0.32	0.29	0.26
12	0.79	0.89	1	0.89	0.8	0.72	0.65	0.59	0.53	0.48	0.43	0.39	0.36	0.32	0.29
16	0.7	0.8	0.89	1	0.9	0.81	0.73	0.66	0.59	0.54	0.49	0.44	0.4	0.36	0.33
20	0.63	0.71	0.8	0.9	1	0.9	0.81	0.73	0.66	0.6	0.54	0.49	0.44	0.4	0.37
24	0.57	0.64	0.72	0.81	0.9	1	0.9	0.81	0.73	0.66	0.6	0.55	0.49	0.45	0.41
28	0.51	0.58	0.65	0.73	0.81	0.9	1	0.9	0.82	0.74	0.67	0.61	0.55	0.5	0.45
32	0.46	0.52	0.59	0.66	0.73	0.81	0.9	1	0.9	0.82	0.74	0.67	0.61	0.55	0.5
36	0.42	0.47	0.53	0.59	0.66	0.73	0.82	0.9	1	0.9	0.82	0.74	0.67	0.61	0.56
40	0.38	0.43	0.48	0.54	0.6	0.66	0.74	0.82	0.9	1	0.91	0.82	0.74	0.68	0.61
44	0.34	0.39	0.43	0.49	0.54	0.6	0.67	0.74	0.82	0.91	1	0.91	0.82	0.75	0.68
48	0.31	0.35	0.39	0.44	0.49	0.55	0.61	0.67	0.74	0.82	0.91	1	0.91	0.82	0.75
52	0.28	0.32	0.36	0.4	0.44	0.49	0.55	0.61	0.67	0.74	0.82	0.91	1	0.91	0.82
56	0.26	0.29	0.32	0.36	0.4	0.45	0.5	0.55	0.61	0.68	0.75	0.82	0.91	1	0.91
60	0.23	0.26	0.29	0.33	0.37	0.41	0.45	0.5	0.56	0.61	0.68	0.75	0.82	0.91	1

Table 0. Instantaneous correlations $\rho(\Delta L_i, \Delta L_j)$ between different LIBORS for $\alpha = 0.9$, $\beta = 0.04$.

$100 \cdot \epsilon_{12}$	(0)	(g)	(g1')	(g1)	(g2)	δ st. E.	$2-\delta$ st. E.
$\leq 0.01\,\%$	0	0	0	0	19	4	0
$\leq 0.02\,\%$	0	0	3	10	47	34	5
$\leq 0.03\,\%$	0	1	10	19	77	73	21
$\leq 0.04\,\%$	0	3	15	34	89	88	41
$\leq 0.05\,\%$	0	8	24	45	91	99	57
$\leq 0.06\,\%$	0	9	32	62	93	100	71
$\leq 0.07\,\%$	0	12	46	79	93	100	75
$\leq 0.08\,\%$	0	13	56	99	96	100	82
$\leq 0.09\,\%$	0	14	71	100	98	100	88
$\leq 0.1\,\%$	0	17	93	100	100	100	93
$\leq 0.2\,\%$	0	41	100	100	100	100	100
$\leq 0.3\,\%$	0	62	100	100	100	100	100
$\leq 0.4\,\%$	0	77	100	100	100	100	100
$\leq 0.5\,\%$	0	89	100	100	100	100	100
$\leq 0.6\,\%$	0	95	100	100	100	100	100
$\leq 0.7\,\%$	0	97	100	100	100	100	100
$\leq 0.8\,\%$	0	97	100	100	100	100	100
$\leq 0.9\,\%$	0	100	100	100	100	100	100
$\leq 1\,\%$	0	100	100	100	100	100	100
$\leq 2\,\%$	0	100	100	100	100	100	100
$\leq 3\,\%$	79	100	100	100	100	100	100
$\leq 4\,\%$	100	100	100	100	100	100	100

Table 1. The cumulative distribution of the relative error ϵ_{12}, for 100 paths under different approximations.

$100 \cdot \epsilon_{24}$	(0)	(g)	(g1')	(g1)	(g2)	δ st. E.	$3-\delta$ st. E.
$\leq 0.01\,\%$	0	0	0	0	3	0	0
$\leq 0.02\,\%$	0	0	0	0	4	17	0
$\leq 0.03\,\%$	0	0	2	0	14	50	0
$\leq 0.04\,\%$	0	0	2	4	20	71	6
$\leq 0.05\,\%$	0	0	4	9	30	91	10
$\leq 0.06\,\%$	0	0	10	11	37	96	15
$\leq 0.07\,\%$	0	2	16	16	47	99	23
$\leq 0.08\,\%$	0	2	17	22	51	99	32
$\leq 0.09\,\%$	0	2	19	24	57	99	48
$\leq 0.1\,\%$	0	3	22	29	66	100	53
$\leq 0.2\,\%$	0	16	59	93	92	100	92
$\leq 0.3\,\%$	0	22	100	98	96	100	99
$\leq 0.4\,\%$	0	34	100	100	99	100	100
$\leq 0.5\,\%$	0	43	100	100	100	100	100
$\leq 0.6\,\%$	0	47	100	100	100	100	100
$\leq 0.7\,\%$	0	60	100	100	100	100	100
$\leq 0.8\,\%$	0	69	100	100	100	100	100
$\leq 0.9\,\%$	0	73	100	100	100	100	100
$\leq 1\,\%$	0	75	100	100	100	100	100
$\leq 2\,\%$	0	98	100	100	100	100	100
$\leq 3\,\%$	0	100	100	100	100	100	100
$\leq 4\,\%$	21	100	100	100	100	100	100
$\leq 5\,\%$	65	100	100	100	100	100	100
$\leq 6\,\%$	91	100	100	100	100	100	100
$\leq 7\,\%$	98	100	100	100	100	100	100
$\leq 8\,\%$	100	100	100	100	100	100	100

Table 2. The cumulative distribution of the relative error ϵ_{24}, for 100 paths under different approximations.

$100 \cdot \epsilon_{36}$	(0)	(g)	(g1')	(g1)	(g2)	δ st. E.	$4-\delta$ st. E.
$\leq 0.01\,\%$	0	0	0	0	0	0	0
$\leq 0.02\,\%$	0	0	0	0	1	17	0
$\leq 0.03\,\%$	0	0	0	0	3	49	1
$\leq 0.04\,\%$	0	0	1	4	4	77	2
$\leq 0.05\,\%$	0	0	1	6	8	89	4
$\leq 0.06\,\%$	0	1	4	9	10	91	6
$\leq 0.07\,\%$	0	1	5	11	13	94	11
$\leq 0.08\,\%$	0	1	7	13	18	98	14
$\leq 0.09\,\%$	0	3	10	16	24	99	24
$\leq 0.1\,\%$	0	3	12	17	30	99	33
$\leq 0.2\,\%$	0	10	33	45	75	100	84
$\leq 0.3\,\%$	0	21	54	87	89	100	94
$\leq 0.4\,\%$	0	25	94	95	92	100	98
$\leq 0.5\,\%$	0	34	96	95	93	100	100
$\leq 0.6\,\%$	0	36	96	96	96	100	100
$\leq 0.7\,\%$	0	40	97	96	96	100	100
$\leq 0.8\,\%$	0	49	98	97	96	100	100
$\leq 0.9\,\%$	0	52	98	98	96	100	100
$\leq 1\,\%$	0	56	99	98	97	100	100
$\leq 2\,\%$	0	89	100	100	100	100	100
$\leq 3\,\%$	1	97	100	100	100	100	100
$\leq 4\,\%$	12	99	100	100	100	100	100
$\leq 5\,\%$	42	100	100	100	100	100	100
$\leq 6\,\%$	75	100	100	100	100	100	100
$\leq 7\,\%$	89	100	100	100	100	100	100
$\leq 8\,\%$	93	100	100	100	100	100	100
$\leq 9\,\%$	97	100	100	100	100	100	100
$\leq 10\,\%$	99	100	100	100	100	100	100

Table 3. The cumulative distribution of the relative error ϵ_{36}, for 100 paths under different approximations.

$100 \cdot \epsilon_{48}$	(0)	(g)	(g1')	(g1)	(g2)	δ st. E.	$4-\delta$ st. E.
$\leq$0.01 %	0	0	0	0	0	6	0
$\leq$0.02 %	0	0	0	0	0	55	0
$\leq$0.03 %	0	0	1	0	0	82	0
$\leq$0.04 %	0	0	2	1	6	90	4
$\leq$0.05 %	0	0	2	4	9	95	12
$\leq$0.06 %	0	0	3	4	13	97	21
$\leq$0.07 %	0	0	7	8	14	97	31
$\leq$0.08 %	0	0	10	12	20	98	41
$\leq$0.09 %	0	0	15	19	21	98	52
$\leq$0.1 %	0	0	16	22	26	99	67
$\leq$0.2 %	0	8	40	46	71	100	89
$\leq$0.3 %	0	17	74	85	83	100	97
$\leq$0.4 %	0	22	93	93	91	100	99
$\leq$0.5 %	0	30	95	94	92	100	100
$\leq$0.6 %	0	35	95	95	95	100	100
$\leq$0.7 %	0	40	96	95	95	100	100
$\leq$0.8 %	0	41	96	96	95	100	100
$\leq$0.9 %	0	45	96	96	96	100	100
$\leq$1 %	0	54	96	96	96	100	100
$\leq$2 %	2	90	100	100	100	100	100
$\leq$3 %	19	97	100	100	100	100	100
$\leq$4 %	55	98	100	100	100	100	100
$\leq$5 %	79	100	100	100	100	100	100
$\leq$6 %	88	100	100	100	100	100	100
$\leq$7 %	95	100	100	100	100	100	100
$\leq$8 %	97	100	100	100	100	100	100
$\leq$9 %	99	100	100	100	100	100	100
$\leq$10 %	100	100	100	100	100	100	100

Table 4. The cumulative distribution of the relative error ϵ_{48}, for 100 paths under different approximations.

3 Direct simulation of log-normal approximations

The results of section (2.2) listed in tables 1-4 clearly show that the lognormal models (0) and (g) are reasonable approximations and the models $(g1')$, $(g1)$ and $(g2)$ are pretty good approximations to the solution of SDE (4). We now present direct techniques for log-normal approximations, in particular we illustrate an effective simulation of the $(g)-$approximation by a lognormal random field in (3.1).

The motivation for direct simulation methods is clear: In contrast to standard numerical solution of stochastic differential equations there is no need for taking small time steps. Indeed, it is possible to construct the solution directly at the desired points in time, e.g., at the points of the given tenor structure $0 < T_1 < T_2 < \ldots < T_n$.[3] It will be shown in section (4) that in many typical applications direct simulation methods take much less computing time.

3.1 Random field simulation of the $(g)-$approximation (RFS)

Due to the simple correlation structure of the $(g)-$approximation it is possible to set up a lognormal random field model by a simulation technique as studied in [8] in a more general setting; we construct a lognormal random field whose first two statistical moments are consistent with those of the $(g)-$approximation.

We thus introduce the lognormal random model

$$\mathcal{L}^{(g)}(i,t) = \exp[\xi^{(g)}(i,t)] \tag{20}$$

[3]From now on, (T_i) is an arbitrary sequence of future time points, so not necessarily $T_i = i\delta$ as in section (2.2).

with Gaussian $\xi^{(g)}(i,t)$, $i=1,\ldots,n-1$, $t_0 \le t \le T_i$, whose mean and covariation structure coincide with that of $\ln(L_i^{(g)}(t)/L_i(t_0))$, $t_0 \le t \le T_i$, $i=1,\ldots n-1$, in the $\mathbb{P}_n-$ measure:

$$\langle \xi^{(g)}(i,t) \rangle = \langle \ln\Big(\frac{L_i^{(g)}(t)}{L_i(t_0)}\Big) \rangle, \tag{21}$$

$$\langle \xi^{(g)}(i_1,t_1), \xi^{(g)}(i_2,t_2) \rangle = \langle \ln\Big(\frac{L_{i_1}^{(g)}(t_1)}{L_{i_1}(t_0)}\Big), \ln\Big(\frac{L_{i_2}^{(g)}(t_2)}{L_{i_2}(t_0)}\Big) \rangle, \tag{22}$$

where the bracket notations $\langle U \rangle$ and $\langle U,V \rangle$ denote $\mathbb{E}_n(U)$ and $\mathbb{E}_n(UV)$ in the $\mathbb{P}_n-$ measure, respectively. From (14) we see that

$$\langle \xi^{(g)}(i,t) \rangle \equiv \mu^{(g)}(i;t_0,t) = -\sum_{j=i+1}^{n-1} \frac{\delta_j L_j(t_0)}{1+\delta_j L_j(t_0)} \int_{t_0}^{t} \boldsymbol{\gamma}_i \cdot \boldsymbol{\gamma}_j(s) ds - \frac{1}{2}\int_{t_0}^{t} |\gamma_i|^2(s) ds, \tag{23}$$

$$\langle \xi^{(g)}(i_1,t_1), \xi^{(g)}(i_2,t_2) \rangle \equiv cov^{(g)}(i_1,i_2;t_0,t_1 \wedge t_2) + \mu^{(g)}(i_1;t_0,t_1)\mu^{(g)}(i_2;t_0,t_2), \tag{24}$$

where

$$cov^{(g)}(i_1,i_2;t_0,t) = \int_{t_0}^{t} \gamma_{i_1} \cdot \gamma_{i_2}(s) ds.$$

We now construct numerically the desired random field $\mathcal{L}^{(g)}(i,T_j)$, $i=1,\ldots,n-1$; $j=1,\ldots i$. To do this, we could simulate the Gaussian vector with the given covariance structure by a conventional simulation technique, see e.g. [8]. However, the specific time correlation (24) resulting from the fact that $\xi^{(g)}$ has independent increments, suggests a different simulation algorithm.

Indeed, in the first step, we simulate a $n-1$-dimensional Gaussian vector $(\xi^{(g)}(1,T_1), \ldots, \xi^{(g)}(n-1,T_1))$ as

$$\xi^{(g)}(i,T_1) = \mu^{(g)}(i;t_0,T_1) + \sum_{k=1}^{K_1} h_{ik}^{(1)} \eta_k^{(1)}, \quad i=1,\ldots,n-1 \tag{25}$$

where the $(n-1)\times K_1$ matrix $[h_{ik}^{(1)}]$ satisfies a Cholesky decomposition

$$\sum_{k=1}^{K_1} h_{ik}^{(1)} h_{jk}^{(1)} = cov^{(g)}(i,j;t_0,T_1), \quad i,j=1,\ldots,n-1; \tag{26}$$

$h_{ik}^{(1)} = 0$ for $i > n-1-K_1+k$, $\{\eta_k^{(1)}\}_{k=1}^{K_1}$ is a set of independent standard Gaussian random numbers and K_1 is the rank of the covariance matrix (26). Note that, in general, $K_1 \le n-1$ and $K_1 = d$; the number of independent Brownian motions in the LIBOR model, in the case where the γ_i are time independent.

In the l-th step $(2 \le l \le n-1)$ we have:

$$\xi^{(g)}(i,T_l) = \xi^{(g)}(i,T_{l-1}) + \mu^{(g)}(i;t_0,T_l) - \mu^{(g)}(i;t_0,T_{l-1}) + \sum_{k=1}^{K_l} h_{ik}^{(l)} \eta_k^{(l)}, \quad i=l,\ldots,n-1, \tag{27}$$

where the $(n-l)\times K_l$ matrix $[h_{ik}^{(l)}]_{i,k=l,\ldots,n-1}$ satisfies a decomposition

$$\sum_{k=1}^{K_l} h_{ik}^{(l)} h_{jk}^{(l)} = cov^{(g)}(i,j;T_{l-1},T_l), \quad i,j=l,\ldots,n-1; \tag{28}$$

$h_{ik}^{(l)} = 0$ for $i > n-1-K_l+k$, $\{\eta_k^{(l)}\}_{k=1}^{K_l}$ is a set of independent standard Gaussian random numbers and K_l is the rank of the covariance matrix (28). So, in general, $K_l \leq n-l$ and $K_l \leq \min(d, n-l)$ in the case where the γ_i are time independent.

After $n-1$ steps we thus find

$$L_i^{(g)}(T_j) = L_i(t_0)\mathcal{L}^{(g)}(i,T_j) = L_i(t_0)\exp\{\xi^{(g)}(i,T_j)\}, \qquad i=1,\ldots,n-1;\ j=1,\ldots,i. \quad (29)$$

Analogously, the same procedure could be easily carried out for the lognormal approximations (0). Indeed, the simulation formulae (25)- (29) remain the same, but the functions $\mu^{(g)}$ and $cov^{(g)}$ should be replaced with

$$\mu^{(0)}(i;t_0,t_1) = 0, \quad \text{and} \quad cov^{(0)}(i_1,i_2;t_0,t) = cov^{(g)}(i_1,i_2;t_0,t),$$

for the $(0)-$approximation.

Remark 3.1.1 Of course, in a random field Monte Carlo simulation all the Cholesky decompositions above can be computed outside of the simulation loop. In general, the cost of the Cholesky decomposition in the $l'-$th step of the random field construction is $\mathcal{O}((n-l)^3)$, so the total cost of the different Cholesky decomposition is $\mathcal{O}(n^4)$. Moreover, in the case where the γ_i are *time independent* it is easily seen that, in fact, only one Cholesky decomposition has to be computed at a cost of $\mathcal{O}(n^3)$. However, for a detailed cost comparison of random field simulation to other direct simulation methods and Euler stepping SDE simulation, see section (4).

3.2 Simulation of the $(g1')$, $(g1)$ and $(g2)$ approximation

We consider the $g1'$-approximation by example as the $(g1)$ and $(g2)$ can be treated analogously. We define,

$$\mu^{(g1')}(i;t_0,t) = -\sum_{j=i+1}^{n-1}\delta_j L_j(t_0)\int_{t_0}^{t}\boldsymbol{\gamma}_i\cdot\boldsymbol{\gamma}_j(s)ds - \frac{1}{2}\int_{t_0}^{t}|\gamma_i|^2(s)ds$$

and from (16) we derive

$$\ln\frac{L_i^{(g1')}(t)}{L_i(t_0)} = \mu^{(g1')}(i;t_0,t) + \int_{t_0}^{t}\left[1-\sum_{j=i+1}^{n-1}\delta_j L_j(t_0)\int_s^t \gamma_j\cdot\gamma_i(u)du\right]\gamma_i(s)\cdot dW_s.$$

We thus have

$$Cov[\xi^{(g1')}(i_1,t_1),\xi^{(g1')}(i_2,t_2)] = \int_{t_0}^{t_1\wedge t_2}\gamma_{i_1}\cdot\gamma_{i_2}(s)\left[1-\sum_{j=i_1+1}^{n-1}\delta_j L_j(t_0)\int_s^{t_1}\gamma_j\cdot\gamma_{i_1}(u)du\right]\times$$
$$\left[1-\sum_{k=i_2+1}^{n-1}\delta_k L_k(t_0)\int_s^{t_2}\gamma_k\cdot\gamma_{i_2}(u)du\right]ds. \quad (30)$$

For the $(g1)$ and $(g2)$-approximation one can derive similar approximations straightforwardly from (16), (17), respectively.

Unfortunately, the covariance functions of $(g1)$, $(g1')$ and $g(2)$ do not have the special structure that the (0) and $(g)-$ approximation do, so a random field construction like in (3.1) does not work. For instance, the increment $\ln L_i(T_l) - \ln L_i(T_{l-1})$ is now in general correlated with $\ln L_i(T_{l-1})$ for $i \geq l-1$. However, it is possible to simulate the desired log-LIBORS simultaneously as one $q-$dimensional random vector ξ. Let the index set $\mathcal{I}$ be the collection of pairs (i,j) for which $L_i(T_j)$, $1 \leq j \leq i \leq n-1$ is to be simulated. So, q is equal to the number of

elements of $\mathcal{I}$ and, for instance, $q = n(n-1)/2$ in case LIBORs over the whole tenor structure are required. Let further $\phi : \mathcal{I} \longrightarrow \{1, \ldots, q\}$ be an arbitrary bijection, then

$$\xi_{\phi(i,j)} := \ln \frac{L_i^{(\cdot)}(T_j)}{L_i(t_0)} = \mu^{(\cdot)}(i; t_0, T_j) + h_{\phi(i,j),1}\eta_1 + \cdots + h_{\phi(i,j),K}\eta_K; \quad (i,j) \in \mathcal{I}, \tag{31}$$

where $(\cdot)$ stands for $(g1')$, $(g1)$, $(g2)$, respectively, the $q \times K$ matrix h satisfies a Cholesky decomposition

$$\sum_{k=1}^{K} h_{pk} h_{lk} = cov^{(\cdot)}(\xi_p, \xi_l) \quad p, l = 1, \ldots, q, \tag{32}$$

$h_{pk} = 0$ for $p > q - K + k$, $\{\eta_k\}_{k=1}^K$ is a set of independent standard Gaussian random numbers and K is the rank of the covariance matrix (32) which, for a specific lognormal approximation, is determined by its covariance structure, for instance, (30).

For a full tenor structure, hence for $\mathcal{O}(n^2)$ log LIBORS, the Cholesky decomposition will now require a computational cost of $\mathcal{O}(n^6)$ and compared to this the cost of the drift terms can be neglected. However, all these computations can be done outside of the simulation loop.

3.3 Cost analysis of Euler SDE simulation and direct simulation methods

Here we give formulae for the cost of Euler SDE simulation, random field simulation of the $(g)-$approximation and the direct simulation method for the other lognormal approximations. We disregard all computations which can be done outside of the Monte Carlo simulation loop such as the computation of various Cholesky decompositions etc.

Let us suppose that we are faced with the simulation of

$$L_i(T_j),\ 1 \le j \le m;\ j \le i \le n-1, \tag{33}$$

for fixed m in the $\mathbb{P}_n-$measure.

3.3.1 Euler scheme for solving the $\log$ –LIBOR SDE system,

$$dY_i = -\sum_{j=i+1}^{n-1} \frac{\delta_j e^{Y_j}}{1+\delta_j e^{Y_j}} \gamma_i \cdot \gamma_j \, dt - \frac{1}{2}|\gamma_i|^2 dt + \ \gamma_i \cdot dW^{(n)}; \quad i = 1, \ldots, n-1, \tag{34}$$

where $Y_i := \ln L_i(t)$. For the volatilities $\gamma_i = (\gamma_{i,1}, \ldots, \gamma_{i,d})$, $1 \le i \le n-1$, we may assume that $\gamma_{i,k} = 0$ for $i > n-1-d+k$ and then it is not difficult to verify that the computation of a single Euler step from t to $t + \Delta t$; $t < T_1$, requires a cost of

$$\begin{aligned} Cost_{Eulerstep}(n,d,1) &= \overbrace{(n-2)(c_* + c_{\dot{-}} + c_+ + c_{\exp}) + \frac{(n-2)(n-1)}{2}(c_* + c_+)}^{computation\ drift\ term} + \\ &\quad \overbrace{+d(c_{\text{rand}} + c_*) + [(n-1-d)d + \frac{d^2+d}{2}](c_* + c_+)}^{computation\ noise\ term} \\ &=: (n-2)\tilde{c}_{\exp} + [\frac{(n-2)(n-1)}{2} + nd - \frac{d^2+d}{2}]\tilde{c}_* + d\tilde{c}_{\text{rand}}, \end{aligned} \tag{35}$$

where the cost of one addition, multiplication, division, exponentiation and the generation of a standard Gaussian random number is denoted by c_+, c_*, $c_{\dot{-}}$, $c_{\exp}$ and c_{rand}, respectively. In

practice $\tilde{c}_* \approx c_*$, $\tilde{c}_{\exp} \approx c_{\exp}$, $\tilde{c}_{\rm rand} \approx c_{\rm rand}$.
From (35) it is obvious that we have in general for $T_{i-1} < t < T_i$; $i \geq 1$, (where $T_0 := t_0$)

$$\begin{aligned} Cost_{Eulerstep}(n,d,i) &= (n-i-1)\tilde{c}_{\exp} + [\frac{(n-i-1)(n-i)}{2} + \max(n-i-d,0)d + \\ &\quad + \frac{\min^2(d,n-i)+\min(d,n-i)}{2}]\tilde{c}_* + \min(d,n-i)\tilde{c}_{\rm rand} \\ &=: \mathcal{C}(d,n-i). \end{aligned} \tag{36}$$

Remark 3.3.1 In our applications n is typically large, e.g. $n \approx 40$, 60 and therefore we could try to deal with asymptotic expression for the behaviour of $\mathcal{C}(d,k)$ for large k and certain d. However, we have to be careful; the cost of the exponential function and the Gaussian random number generator is considerably higher than the cost of a multiplication. For the compiler we used we found by experiment $c_{\exp}/c_* \approx 25$ and with this compiler we found for the random number generator we used, $c_{\rm rand}/c_* \approx 10$. So in a typical situation, for instance $k \approx 40$, 60, the term involving $c_{\exp}$ in (36) can not be neglected at all and the same is true for the term involving $c_{\rm rand}$ when $d = n-1$ (a full factor model). Therefore, it is important to consider (36) for all k, rather than for $k \to \infty$ only.

Obviously, (36) yields,

$$\begin{aligned} \mathcal{C}(d,k) &= (k-1)\tilde{c}_{\exp} + k^2\tilde{c}_* + k\tilde{c}_{\rm rand}; \qquad k < d, \\ \mathcal{C}(d,k) &= (k-1)\tilde{c}_{\exp} + [\frac{(k-1)k}{2} + (k-d)d + \frac{d^2+d}{2}]\tilde{c}_* + d\tilde{c}_{\rm rand}; \qquad k \geq d \end{aligned} \tag{37}$$

The numerical experiments in (2.2) have shown that, in practice, for a uniform tenor structure it is accurate enough to take time steps of order $\Delta t = \delta, 2\delta$ for time t up to T_1 and between two tenors T_i, T_{i+1} we take δ_i for the Euler step size. So, it is clear that the total cost of a thus organized SDE simulation of one sample of the values (33) will be equal to

$$Cost_{SDE}(n,d,m) = \frac{T_1}{\Delta t} Cost_{Euler\ step}(n,d,1) + \sum_{i=2}^{m} Cost_{Euler\ step}(n,d,i) + Cost^{(m)}_{Exp.\ calls}, \tag{38}$$

where $Cost^{(m)}_{Exp.\ calls}$ takes into account the cost of the exponential calls at T_m to get LIBORs rather than $\log-$LIBORs. For $i < m$ these exponential calls are already included in the first and second term of (38) as LIBORs at T_i are needed in the drift terms. Hence,

$$Cost_{SDE}(n,d,m) = \frac{T_1}{\Delta t}\mathcal{C}(d,n-1) + \sum_{k=n-m}^{n-2} \mathcal{C}(d,k) + (n-m)\tilde{c}_{\exp} \tag{39}$$

with empty sums defined as zero. We derive from (37) and (39) by elementary algebra[4] explicit expressions for the cost of the Euler method for $m > n-d$ and $m \leq n-d$, respectively:

$$\begin{aligned} Cost_{SDE}(n,d,m) &= \frac{T_1}{\Delta t}\{(n-2)\tilde{c}_{\exp} + [\frac{(n-2)(n-1)}{2} + nd - \frac{d^2+d}{2}]\tilde{c}_* + d\tilde{c}_{\rm rand}\} + \\ &\quad + \{(n-1)m - \frac{m^2+3m-4}{2}\}\tilde{c}_{\exp} + \{-\frac{n^3}{6} + \frac{2m+d-1}{2}n^2 + \\ &\quad - \frac{6m^2+6m+3d^2+6d-10}{6}n + \frac{2m^3+3m^2+m+d^3+3d^2+2d-6}{6}\}\tilde{c}_* + \\ &\quad \{-\frac{n^2}{2} + \frac{2m+2d+1}{2}n - \frac{m^2+m+d^2+3d}{2}\}\tilde{c}_{\rm rand}; \ m > n-d \ \text{ and} \end{aligned} \tag{40}$$

[4]The expressions (40) and (41) can be checked easily with Mathematica or Maple, for instance.

$$
\begin{aligned}
Cost_{SDE}(n,d,m) &= \frac{T_1}{\Delta t}\{(n-2)\tilde{c}_{\exp} + [\frac{(n-2)(n-1)}{2} + nd - \frac{d^2+d}{2}]\tilde{c}_* + d\tilde{c}_{\text{rand}}\} + \qquad (41)\\
&+\{(n-1)m - \frac{m^2+3m-4}{2}\}\tilde{c}_{\exp} + \{\frac{m-1}{2}n^2 - \frac{m^2+2m-2md+2d-3}{2}n + \\
&+\frac{m^3+3m^2+2m-6-3d^2m-3dm^2+3d^2+3d}{6}\}\tilde{c}_* + (m-1)d\tilde{c}_{\text{rand}};\ m \le n-d.
\end{aligned}
$$

The expressions (40) and (41) will be used later for a cost comparison of random field simulation and direct simulation of different lognormal approximations with Euler SDE simulation in various situations.

3.3.2 Random field simulation technique.

Here we consider the general case where γ is time dependent and we thus have to take in (27), $K_l = n - l$ for $1 \le l \le n$, even if d is small. We choose the $(n-l)\times(n-l)$-matrix $h^{(l)}$ in (27) as an upper-triangular matrix. Disregarding again pre-computation costs outside of the Monte Carlo loop it follows from (27) that the cost of calculating one sample of the LIBORs (33) is given by

$$
\begin{aligned}
Cost_{RFS}(n,m) &= \sum_{l=1}^{m}\{\frac{1}{2}(n-l)(n-l+1)\tilde{c}_* + (n-l)\tilde{c}_{\text{rand}}\} + Cost^{(m,n)}_{Exp.\ calls}\\
&= \frac{1}{6}(3mn^2 - 3m^2n + m^3 - m)\tilde{c}_* + \frac{1}{2}m(2n-m-1)(\tilde{c}_{\text{rand}} + \tilde{c}_{\exp}), \qquad (42)
\end{aligned}
$$

where the term $Cost^{(m,n)}_{Exp.\ calls} = \frac{1}{2}m(2n-m-1)\tilde{c}_{\exp}$ is taken into account because we need LIBORs rather than $\log-$LIBORs.

Remark 3.3.2 It turns out in practice that it is very reasonable to take γ_i piece-wise constant between the tenors: $\gamma_i(s) = \gamma_i^{(p)}$ for $T_p \le s < T_{p+1}$, $1 \le p \le n-1$. In this situation the first Cholesky decomposition in the random field construction, (26), might have rank $n-1$, but for the Cholesky decompositions in step $2 \le l \le n-1$ we may take $K_l = \min(d, n-l)$. In this important practical situation the random field simulation will be much faster in case d is small. Indeed, it is easily verified that for the computation cost we now have

$$
\begin{aligned}
Cost^{\gamma\,p.c.[T_1,T_n]}_{RFS}(n,d,m) &\le \frac{1}{2}n(n-1)\tilde{c}_* + (n-1)\tilde{c}_{\text{rand}} + \sum_{l=2}^{m}[(n-l)d\tilde{c}_* + d\tilde{c}_{\text{rand}}] + Cost^{(m,n)}_{Exp.\ calls}\\
&= \frac{1}{2}n(n-1)\tilde{c}_* + (n(m-1) - \frac{m^2+m-2}{2})d\tilde{c}_*\\
&\quad +(n+md-d-1)\tilde{c}_{\text{rand}} + \frac{1}{2}m(2n-m-1)\tilde{c}_{\exp} \qquad (43)
\end{aligned}
$$

Even for a full tenor structure $m = n-1$, we have

$$
\begin{aligned}
Cost^{\gamma\,p.c.[T_1,T_n]}_{RFS}(n,d,m=n-1) &\le (\frac{n^2-n}{2} + \frac{n^2-3n+2}{2}d)\tilde{c}_* +\\
&\quad +(n(d+1) - 2d - 1)\tilde{c}_{\text{rand}} + \frac{1}{2}n(n-1)\tilde{c}_{\exp}, \qquad (44)
\end{aligned}
$$

and so the coefficients of $\tilde{c}_*$, $\tilde{c}_{\text{rand}}$ and $\tilde{c}_{\exp}$ in (43) and (44) are for small d quadratic and linear in n, respectively, whereas the corresponding coefficients in the cost of the SDE simulation tend to be larger: For example, when $m = n-1$ in (40) the coefficient of $\tilde{c}_*$ still contains $n^3/6$ and

$\frac{T_1}{\Delta t}\frac{n^2}{2}$ for small d.
If, moreover, γ_i is constant on $[t_0, T_1[$, i.e. $\gamma_i(s) = \gamma_i^{(0)}$ for $t_0 \leq t < T_1$, a rank-d Cholesky decomposition applies to the $\xi^{(g)}(T_1)$ construction also and then we have

$$\begin{aligned} Cost_{RFS}^{\gamma\, p.c.[t_0,T_n]}(n,d,m) &\leq \sum_{l=1}^{m}[(n-l)d\tilde{c}_* + d\tilde{c}_{\text{rand}}] + Cost_{Exp.\ calls}^{(m,n)} \\ &= (nm - \frac{m^2+m}{2})d\tilde{c}_* + md\tilde{c}_{\text{rand}} + \frac{1}{2}m(2n-m-1)\tilde{c}_{\text{exp}}, \quad (45) \end{aligned}$$

which means a next speed up with respect to Euler SDE simulation in the case where $d << n$; e.g. compare (45) with (41) for $d = 1$.

3.3.3 Direct simulation of the $(g1')$, $(g1)$, and $(g2)-$approximation.

By taking $q = \sum_{j=1}^{m}(n-j) = \frac{1}{2}m(2n-m-1)$ in (31) we see that with an upper-triangular h, for the full rank case $K = q$, the simulation of one sample of (33) will cost inside of the loop:

$$\begin{aligned} Cost_{DS}(n,m) &= \frac{1}{2}q(q+1)\tilde{c}_* + q\tilde{c}_{\text{rand}} + Cost_{Exp.\ calls}^{(m,n)} \\ &= \{\frac{m^2}{2}n^2 - \frac{m^3+m^2-m}{2}n + \frac{m(m+1)(m^2+m-2)}{8}\}\tilde{c}_* + \\ &\quad + \frac{1}{2}m(2n-m-1)(\tilde{c}_{\text{rand}} + \tilde{c}_{\text{exp}}). \quad (46) \end{aligned}$$

It is clear that for $m = n-1$ the first term will be of order $\mathcal{O}(n^4 c_*)$ and so, direct simulation of the $(g1')$, $(g1)$, or $(g2)-$approximation for a full tenor structure $(m = n-1)$ can only be recommended when n is not too large, whereas for larger n this simulation method is recommended for relatively small values of m. For example, $m = 1$ in (46) yields

$$Cost_{DS}(n, m=1) = \frac{n^2-n}{2}\tilde{c}_* + (n-1)(\tilde{c}_{\text{rand}} + \tilde{c}_{\text{exp}}). \quad (47)$$

4 Efficiency gain with respect to SDE simulation; an optimal simulation program

Let us suppose that we are faced with a Monte Carlo evaluation of a LIBOR derivative involving LIBORs specified in (33). Rather than full Euler stepping from the starting date t_0, it may be profitable to simulate $L(T_1)$ by one of the lognormal approximation and then, for instance, proceed with Euler stepping through the remaining tenors, of course, provided that $L(T_1)$ is well approximated. Alternatively, provided the (g)-approximation is tolerable, one may apply the random field simulation technique. It is to expect that for longer dated products (i.e. larger T_1) and in particular when additionally m is small, e.g. $m = 1$ in the case of a European style derivative, both alternatives may yield a substantial efficiency gain. We will compute the order of this gain for a "full" tenor structure, i.e. $m = n-1$ and the European case $m = 1$, where we distinguish between the multi-factor case $d = n-1$ and the one factor case $d = 1$.

1: Lognormal approximation of $L(T_1)$ followed by Euler stepping

As a first alternative to full Euler stepping we thus consider a simulation algorithm which simulates with a proper lognormal approximation the LIBORs $L(T_1)$ first and then proceeds with

Euler δ-stepping. By the results of section (3.3) we may compute for this method straightforwardly the efficiency ratio

$$R^{(\mathbf{1})}_{\text{Eff}}(n,d,m) := \frac{Cost_{SDE_{[t_0,T_m]}}}{Cost_{DS_{[t_0,T_1]}\&SDE_{[T_2,T_m]}}}$$

and yield the following results:

full structure, multi-factor

$$R^{(\mathbf{1})}_{\text{Eff}}(n,n-1,n-1) \approx \frac{(n\frac{T_1}{\Delta t}+\frac{n^2}{2})\tilde{c}_{\exp}+(n\frac{T_1}{\Delta t}+\frac{n^2}{2})\tilde{c}_{\text{rand}}+(n^2\frac{T_1}{\Delta t}+\frac{n^3}{3})\tilde{c}_*}{\frac{n^2}{2}\tilde{c}_{\exp}+\frac{n^2}{2}\tilde{c}_{\text{rand}}+\frac{n^3}{3}\tilde{c}_*}$$

full structure, one factor

$$R^{(\mathbf{1})}_{\text{Eff}}(n,1,n-1) \approx \frac{(n\frac{T_1}{\Delta t}+\frac{n^2}{2})\tilde{c}_{\exp}+(\frac{T_1}{\Delta t}+n)\tilde{c}_{\text{rand}}+(\frac{n^2}{2}\frac{T_1}{\Delta t}+\frac{n^3}{6})\tilde{c}_*}{\frac{n^2}{2}\tilde{c}_{\exp}+2n\tilde{c}_{\text{rand}}+\frac{n^3}{6}\tilde{c}_*+}$$

European, multi-factor

$$R^{(\mathbf{1})}_{\text{Eff}}(n,n-1,1) \approx \frac{(n\frac{T_1}{\Delta t}+n)\tilde{c}_{\exp}+n\frac{T_1}{\Delta t}\tilde{c}_{\text{rand}}+n^2\frac{T_1}{\Delta t}\tilde{c}_*}{n\tilde{c}_{\exp}+n\tilde{c}_{\text{rand}}+\frac{n^2}{2}\tilde{c}_*}$$

European, one factor

$$R^{(\mathbf{1})}_{\text{Eff}}(n,1,1) \approx \frac{(n\frac{T_1}{\Delta t}+n)\tilde{c}_{\exp}+\frac{T_1}{\Delta t}\tilde{c}_{\text{rand}}+\frac{n^2}{2}\frac{T_1}{\Delta t}\tilde{c}_*}{n\tilde{c}_{\exp}+n\tilde{c}_{\text{rand}}+\frac{n^2}{2}\tilde{c}_*}$$

Hence, when $\frac{T_1}{\Delta t} \gtrsim n$ it is clear that this alternative will be substantially faster than full Euler stepping.

2: Random field simulation

When volatilities are not too high or T_m is not too large the $(g)-$approximation might be acceptable and then, particularly for a full tenor structure ($m = n-1$), it might be profitable to use the random field simulation technique. The efficiency ratio

$$R^{(\mathbf{2})}_{\text{Eff}}(n,d,m) := \frac{Cost_{SDE_{[t_0,T_m]}}}{Cost_{RFS_{[T_1,T_m]}}}$$

may be computed by section (3.3) again and for $m = n-1$ we have

full structure, multi-factor

$$R^{(\mathbf{2})}_{\text{Eff}}(n,n-1,n-1) \approx \frac{(n\frac{T_1}{\Delta t}+\frac{n^2}{2})\tilde{c}_{\exp}+(n\frac{T_1}{\Delta t}+\frac{n^2}{2})\tilde{c}_{\text{rand}}+(n^2\frac{T_1}{\Delta t}+\frac{n^3}{3})\tilde{c}_*}{\frac{n^2}{2}\tilde{c}_{\exp}+\frac{n^2}{2}\tilde{c}_{\text{rand}}+\frac{n^3}{6}\tilde{c}_*}$$

full structure, one factor

$$R^{(\mathbf{2})}_{\text{Eff}}(n,1,n-1) \approx \frac{(n\frac{T_1}{\Delta t}+\frac{n^2}{2})\tilde{c}_{\exp}+(\frac{T_1}{\Delta t}+n)\tilde{c}_{\text{rand}}+(\frac{n^2}{2}\frac{T_1}{\Delta t}+\frac{n^3}{6})\tilde{c}_*}{\frac{n^2}{2}\tilde{c}_{\exp}+\frac{n^2}{2}\tilde{c}_{\text{rand}}+\frac{n^3}{6}\tilde{c}_*},$$

from which we conclude that, in general, the efficiency gain with respect to simulation alternative **(1)** is limited: If in the full rank case $n^3\tilde{c}_*$ is much larger than $n^2\tilde{c}_{\exp}$, random field simulation is about two times faster than simulation alternative **(1)**. However, for a low factor model with $\gamma(s)$ piece wise constant between T_1 and T_n it follows from remark (3.3.2) that random field simulation is really faster than alternative **(1)**. In the one factor case we then have

full structure, one factor

$$R^{(\mathbf{2}),\ \gamma\ \text{p.c.}}_{\text{Eff}}(n,1,n-1) \approx \frac{(n\frac{T_1}{\Delta t}+\frac{n^2}{2})\tilde{c}_{\exp}+(\frac{T_1}{\Delta t}+n)\tilde{c}_{\text{rand}}+(\frac{n^2}{2}\frac{T_1}{\Delta t}+\frac{n^3}{6})\tilde{c}_*}{\frac{n^2}{2}\tilde{c}_{\exp}+2n\tilde{c}_{\text{rand}}+n^2\tilde{c}_*}.$$

For any problem in practice for which alternatives **(1)** or **(2)** applies it will be easy to compute or estimate from the expressions in section (3.3) the efficiency gain with respect to Euler stepping SDE simulation. However, instead of listing many possibilities we rather present typical situations in which the proposed simulation alternatives improve upon standard Euler stepping.

Example 4.0.3 Suppose we have to price a relatively long term LIBOR option with $T_1 = 12$ years, $T_n = 22$ years, 3 month periods and where LIBORs over the full tenor structure are required for the valuation of the contract ($m = n-1$). A product of this type is, for instance, the trigger swap, see section (5). So, $\delta = 0.25$, $n = 41$, $m = 40$. For our C++ compiler the relative cost of a standard Gaussian random number and the exponential function is approximately $\tilde{c}_{\text{rand}}/\tilde{c}_* \approx 10$ and $\tilde{c}_{\exp}/\tilde{c}_* \approx 25$, respectively.

The relative cost of full Euler $\delta-$stepping from t_0 to T_n with respect to simulation method **(1)**: $(g2)-$approximation of $L(T_1)$ and Euler $\delta-$stepping from T_2 to T_n,

$$R^{(\mathbf{1})}_{\text{Eff}} := \frac{Cost_{SDE_{[t_0,T_n]}}}{Cost_{DS_{[t_0,T_1]}\&SDE_{[T_2,T_n]}}},$$

is computed from expressions in section (3.3) and listed in table 5 for a one and two factor model, a multi factor model and different Euler step sizes, $\Delta t = \delta, 2\delta, 3\delta$ on $[t_0, T_1]$. The absolute computation costs of the SDE method in terms of 10^4 multiplications is given in brackets [5].

$R^{(\mathbf{1})}_{\text{Eff}}$ $(Cost_{SDE} \times 10^4 \tilde{c}_*)$

Δt	$d = 1$	$d = 2$	$d = 40$
δ	3.66 (11.6)	3.64 (12.0)	3.83 (19.0)
2δ	2.30 (7.0)	2.29 (7.5)	2.39 (11.8)
3δ	1.84 (5.8)	1.84 (6.0)	1.90 (9.4)

Table 5

Example 4.0.4 We consider the same problem as in example (4.0.3) except that now only $L_i(T_1)$; $i = 1, \ldots, n-1$ are required for pricing the product, so now $m = 1$. For instance, the swaption and the callable reverse floater are products of this type, see for details section (5). The computed cost ratios of direct simulation of the $(g1), (g1')$ or $(g2)-$approximation with respect to Euler stepping SDE simulation are listed in table 7 for different step sizes Δt and different d. It is clear that the efficiency gain is tremendous in this case. Note that in general when $m = 1$, the simulation costs inside the loop of the $(g)-$ approximation and the $(g1), (g1')$ or $(g2)-$approximation coincide and so a refined lognormal approximation as a $(g1')$, $(g1)$ or $(g2)-$approximation should be prefered in any case.

R_{Cost} $(Cost_{SDE} \times 10^4 \tilde{c}_*)$

Δt	$d = 1$	$d = 2$	$d = 40$
δ	39.5 (8.7)	40.6 (8.9)	64.8 (14.3)
2δ	19.9 (4.3)	20.6 (4.5)	32.6 (7.1)
3δ	13.4 (2.9)	13.8 (3.0)	21.9 (4.8)

Table 6

4.1 An optimal simulation program

Based on the experimental results with respect to the accuracy of different LIBOR approximations in section (2.2) and the cost comparison between standard Euler δ-stepping and different alternative simulation methods in section (4), we now propose the following procedure for the price simulation of a derivative structure involving a system (33) of LIBORs, in a given calibrated LIBOR model.

[5] The approximate expressions in section (4) give nearly the same results.

Step (I): Compare the accuracy of different lognormal approximation for the calibrated LIBOR model by using a path simulation program as designed in section (2.2).
Step (II): Decide which approximations are acceptable in view of the accuracy required for the derivative structure and then follow one of the following alternatives:
Case **(1):** *If the $(g1), (g1')$ or $(g2)-$approximation is tolerable up to $L(T_1)$ while the $(g)-$approximation is not, generate $L(T_1)$ by a direct simulation method of (3.2) and proceed to T_m with Euler $\delta-$stepping.*
Case **(2):** *If the $(g)-$ approximation is tolerable over all tenors, the number of factors (d) is small, and $\gamma(s)$ is piece-wise constant between T_1 and T_m, then apply the random field simulation technique (3.1).*
Case **(3):** *If* **(1)** *and* **(2)** *don't apply, SDE simulation by $\delta-$stepping Euler turns out to be acceptable in almost all practical situations.*

5 Examples of LIBOR derivatives

We now present some test results on the valuation of the swaption and the trigger swap and discuss the pricing of a callable reverse floater.

5.0.1 European swaption

The value of a payer swaption with maturity T_1, strike κ and principal \$1 gives the right to contract at T_1 to pay a fixed coupon κ and receive the $T1-$swap rate at the settlement dates $T_2, .., T_n$. As, equivalently, one can contract for receiving spot LIBOR instead of the $T1-$swap rate, the price of the swaption at $t < T_1$ can be given by

$$Swpn(t) = B_1(t)\mathbb{E}_1\left[\left(\sum_{j=1}^{n-1} B_{j+1}(T_1)\mathbb{E}_{j+1}[(L_j(T_j)-\kappa)\delta_j \mid \mathcal{F}_{T_1}]\right)^+ |\mathcal{F}_t\right],$$

where $(\cdot)^+ := \max(\cdot, 0)$, see [2, 10]. By a martingale property and measure transformation the swaption can be represented in the $\mathbb{P}_n$ measure by

$$Swpn(t) = \sum_{j=1}^{n-1} B_n(t)\mathbb{E}_n\left[\frac{B_{j+1}(T_1)}{B_n(T_1)} 1_A (L_j(T_1)-\kappa)\delta_j \ |\mathcal{F}_t\right]. \tag{48}$$

In (48), A denotes the $\mathcal{F}_{T_1}$ measurable event $\{S(T_1) > \kappa\}$, where the swap rate $S(T_1)$ is given by

$$S(T_1) := \frac{1-B_n(T_1)}{\sum_{k=1}^{n-1}\delta_k B_{k+1}(T_1)} = \frac{-1+\prod_{k=1}^{n-1}(1+\delta_k L_k(T_1))}{\sum_{k=1}^{n-1}\delta_k \prod_{i=k+1}^{n-1}(1+\delta_i L_i(T_1))}$$

and $B_{j+1}(T_1)/B_n(T_1)$ can be expressed in the LIBORs by

$$\frac{B_{j+1}(T_1)}{B_n(T_1)} = \prod_{i=j+1}^{n-1}(1+\delta_i L_i(T_1)).$$

The value of an at the money swaption based on the tenor structure given in example (4.0.4) is simulated for the various LIBOR approximations and the results are listed in table 8. In order to estimate the systematic error in the swaption value due to a particular approximation, the swaption value is simulated by the $\log-$SDE of the approximation, where the same Wiener processes are used for all approximations.

"true value"	$\delta-$step E.	$3\delta-$step E.	$(g2)$	$(g1)$	$(g1')$	(g)	(0)
0.037907	0.037954	0.038071	0.038169	0.037933	0.037728	0.040818	0.05164
syst. err.	0.12%	0.43%	0.69%	0.07%	-0.47%	7.7%	36.2%

Table 8: Swaption values for different LIBOR approximations simulated under the same Wiener processes; $T_1 = 12$, $n = 41$, $\delta_i \equiv 0.25$, $L_i(0) \equiv 0.06045$, $|\gamma_i| \equiv 0.15$, $\alpha = 0.9$, $\beta = 0.04$, $\kappa = 0.06045$. Number of trajectories: 50000, Monte Carlo error (1 standard deviation) ≈ 0.0005 $\approx 1.3\%$; SDEs simulated with $\Delta t = 0.05$.

We note that while the $(g2)-$approximation according to tables 1-4 looks to be the best path-wise lognormal approximation overall, it produces larger outliers than $(g1)$ and $(g1')$. For this reason, apparently, the $(g2)-$approximation does not give an essentially better swaption approximation than the $(g1)$ gives. Further we note that by using a much faster direct simulation method the "real time" Monte Carlo error can be reduced considerably by increasing the number of simulations. For instance, a run of 500000 direct simulations of the $(g1)-$approximation takes, for this example, about 10 seconds on a 500Mhz Unix-workstation and gives a Monte Carlo error of about 0.4%, whereas from table 7 (full rank column) we see that even a $3\delta-$stepping Euler method, which is comparable to $(g1')$ in accuracy, would have taken about 40 times longer.

5.0.2 Trigger swap

Next we consider an up and out trigger swap contract with discretely monitored trigger variable $L_i(T_i)$ and trigger levels $K_1, \ldots, K_n$: As soon as $L_i(T_i) > K_i$ one has to swap LIBOR against a fixed coupon κ for the remaining period $[T_i, T_n]$ with settlement dates $T_{i+1}, \ldots, T_n$.

The value of the trigger swap in the $\mathbb{P}_n$ measure can be expressed by

$$Trswp(t) = \sum_{p=1}^{n-1} B_n(t) \mathbb{E}_n \left[1_{[\tau=p]} \frac{1}{B_n(T_p)} \left(1 - B_n(T_p) - \kappa \sum_{j=p}^{n-1} B_{j+1}(T_p)\delta_j \right) \mid \mathcal{F}_t \right], \qquad (49)$$

where τ, the trigger index, is given by $\tau := \min_{1 \le p < n}\{p \mid L_p(T_p) > K_p\}$, see [10]. In (49) the expression inside the expectation can be expressed in LIBORs only and we thus have

$$Trswp(t) = \sum_{p=1}^{n-1} B_n(t) \mathbb{E}_n \left[1_{[\tau=p]} \left(-1 + \prod_{i=p}^{n-1} (1 + \delta_i L_i(T_p)) - \kappa \sum_{j=p}^{n-1} \delta_j \prod_{i=j+1}^{n-1} (1 + \delta_i L_i(T_p)) \right) \mid \mathcal{F}_t \right]. \qquad (50)$$

As an application of example (4.0.3) we simulate the value of a trigger swap under different LIBOR approximations, just as in the swaption example. The trigger levels are taken to be equal; ; $K_i \equiv 0.08$, see table 9.

"true value"	$\delta-$step E.	$(g2)$	$(g1)$	$(g1')$	(g)	(0)
0.042851	0.042909	0.043184	0.042946	0.042758	0.046142	0.056714
syst. err.	0.13%	0.77%	0.22%	-0.22%	7.6%	32.3%

Table 9: Values of a trigger swap for different LIBOR approximations simulated under the same Wiener processes; $T_1 = 12$, $n = 41$, $\delta_i \equiv 0.25$, $L_i(0) \equiv 0.06045$, $|\gamma_i| \equiv 0.15$, $\alpha = 0.9$, $\beta = 0.04$, $\kappa = 0.06045$, $K_i \equiv 0.8$. Number of trajectories: 25000, Monte Carlo error (1 standard deviation) $\approx 0.0007 \approx 1.6\%$; SDEs simulated with $\Delta t = 0.05$.

Again we see that the $(g2)-$approximation does not give an essentially better result than the $(g1)-$ or $(g1')-$approximation for the same reason as in the swaption example. Regarding the rather large systematic error of the $(g)-$approximation over a ten year time period, for

the example trigger swap above we propose a direct simulation method (4.1)-*(i)* by using the $(g1)-$approximation. On our 500 Mhz workstation a run of 100000 simulations by method (4.1)-*(i)* of the (full factor) LIBOR model takes about 4 minutes and yields a tolerable Monte Carlo error of about 0.8%, whereas a $\delta-$step Euler method takes about 4 times longer according to table 5. Moreover, although the systematic error of the $\delta-$step Euler method is smaller than the error of the $(g1)-$approximation, the later error is still much smaller than the Monte Carlo error in this case and so the $\delta-$step Euler method will not give an essentially better result.

5.0.3 Callable reverse floater

Note that particularly for products where example (4.0.4) applies the efficiency gain of the proposed simulation method compared with Euler stepping is quite big. A realistic example of such a product is a T_1-*callable reverse floater*, which is a European call option on a reverse floater at T_1. Generally, reverse floaters occur in different variations. As a typical example, [4], the cash flows may be specified by $C_{T_{i+1}} := \delta_i L_i(T_i) - \delta_i \max(K - L_i(T_i), 0)$, $1 \leq i \leq n-1$. By standard financial pricing techniques, [2, 4, 7], it follows that the value of this product at time $t \leq T_1$ is given by

$$\begin{aligned} RF(t) &= B_n(t)\mathbb{E}_n\left(\sum_{i=1}^{n-1}\frac{C_{T_{i+1}}}{B_n(T_{i+1})}|\mathcal{F}_t\right) \\ &= B_1(t) - B_n(t) - \sum_{i=1}^{n-1} B_{i+1}(t)\mathbb{E}_{i+1}[\delta_i \max(K - L_i(T_i), 0)|\mathcal{F}_t] \end{aligned} \tag{51}$$

and can be evaluated analytically in a LIBOR market model, in which $L_i(T_i)$ is log-normally distributed under $\mathbb{P}_{i+1}$. Hence $RF(T_1)$ may be expressed explicitly as a function of $L(T_1)$ and it is possible to compute the price of the callable reverse floater,

$$CRF(t) := B_n(t)\mathbb{E}_n\left[\tfrac{RF(T_1)^+}{B_n(T_1)}|\mathcal{F}_t\right], \tag{52}$$

by Monte Carlo simulation of $L(T_1)$ in the terminal measure. Hence (4.0.4) applies. Moreover, for moderate maturities T_1 the efficiency gain for this product will still be large. From (51) it is clear that this product exhibits both cap and swaption characteristics and thus can not be priced analytically in a LIBOR market model, nor in a swap market model. More technical details around the callable reverse floater can be found in [10].

6 Conclusions

From tables 1-4 in section (2.2) and the examples (5.0.1) and (5.0.2) we conclude that application of the lognormal $(g)-$approximation as proposed by Brace et al., [2], in the valuation of long maturity derivative structures may lead to intolerable errors in the option values. In section (2) different lognormal approximation are constructed, in particular, besides the (0) and $(g)-$approximation we considered the $(g1')$ $(g1)$ and $(g2)-$approximation. While the $(g)-$approximation is not reliable for longer maturity structures, the refined lognormal approximations $(g1')$ $(g1)$ and $(g2)$ are in most cases still acceptable in the sense that the systematic errors in the option values caused by these approximations are well within an in practice for over the counter options thoroughly tolerable Monte Carlo error of about 1%. In view of the larger outliers produced by the $(g2)-$approximation, however, the $(g1)-$approximations seems to be the best candidate in practice and its implementation according to one of the simulation strategies outlined in section (4.1) turns out to be very efficient compared to standard simulation

of the log −LIBOR SDEs with time steps δ, 2δ or 3δ. Moreover, the efficiency gain becomes really tremendous when the proposed simulation method is applied to products which fit into (4.0.4), for instance, the callable reverse floater. Then, for practical purposes we suggest the implementation of a path comparison method as described in section (2.2) as a measuring instrument which helps to decide in a particular situation whether a certain lognormal approximation is acceptable or not. Finally, it should be noted that smile effects are not taken into account in this paper and the extension of the methods presented in this paper to extended LIBOR market models as studied by Andersen, Andreasen, [1], in order to incorporate volatility skews, would be a next interesting research issue.

References

[1] Andersen, L., and Andreasen, J.: Volatility Skews and Extensions of the LIBOR Market model. Working Paper, General Re Financial Products, (1998).

[2] Brace, A., Gatarek, D., Musiela, M.: The Market Model of Interest Rate Dynamics. *Mathematical Finance,* 7 (2), 127-155, (1997).

[3] Curnow, R.N., Dunnett, C.W.: The numerical evaluation of certain multivariate normal integrals. *Ann. Math. Statist.,* (33), 571-579, (1962).

[4] Jamshidan, F.: LIBOR and swap market models and measures. *Finance and Stochastics,* (1), 293-330, (1997).

[5] Kloeden, P.E., Platen, E.: *Numerical Solution of Stochastic Differential Equations.* Springer Verlag, Series Applications of Mathematics, Nr. 23 1992.

[6] Miltersen, K.R., Sandmann, K., and Sondermann, D.: Closed-form Solutions for Term Structure Derivatives with Lognormal Interest Rates. *J. Finance*, (52), 409-430, (1997).

[7] Musiela, M. and Rutkowski, M.: Continuous-Time Term Structure models: Forward Measure Approach. *Finance and Stochastics*, (1), 261-292, (1997).

[8] Sabelfeld, K.K.: *Monte Carlo methods in boundary value problems.* Springer-Verlag, (1991).

[9] Schoenmakers, J.G.M., Heemink, A.W.: Fast Valuation of Financial Derivatives. *Journal of Computational Finance*, first issue, (1997).

[10] Schoenmakers, J.G.M., Coffey, B.: LIBOR rate models, related derivatives and model calibration. Preprint no. 480, Weierstrass Institute Berlin, (1999).

[11] Schoenmakers, J.G.M., Coffey, B.: Stable implied calibration of a multi-factor LIBOR model via a semi-parametric correlation structure. Preprint no. 611, Weierstrass Institute Berlin, (1999).

[12] Sidenius, J.: LIBOR market models in practice. Skandinaviska Enskilda Banken, Copenhagen, (1997).